

Influence of Soil Layers on the Infiltration Rates and Cumulative Infiltration Using Modified Green Ampt Model in the HYDROL-INF Simulation Environment

Mosammat Mustari Khanaum^{1*}, Md. Saidul Borhan²

¹ Graduate Research Assistant, Civil, Construction and Environmental Engineering, North Dakota State University, 1410 North 14th Ave, Fargo, ND 58102, USA.

² Environmental Specialist, Texas Department of Transportation, Maintenance Division, TxDOT, 6230 E. Stassney Lane, Austin, TX 78744, USA.

* Corresponding author's e-mail: mosammat.khanaum@ndsu.edu

ABSTRACT

Soil profiles are generally heterogeneous and consist of various horizontal layers due to geological processes, the formation of crusts, or other artificial or man-made activities. To quantify infiltration into these heterogeneous soil profiles, the Modified Green-Ampt Model (MGAM) is a physically-based hydrologic model that can efficiently perform under both steady and unsteady rainfall events. Based on the secondary data, this study sought to determine the effect of changing soil layers (soil textures) on infiltration rates and cumulative infiltrations in both laboratory and field settings. Different scenarios were analyzed by rearranging soil layers and evaluating their impacts on corresponding infiltration rates and cumulative infiltrations. Simulations were run with HYDROL-INF software environment using MGAM. Three scenarios were considered for a laboratory experiment with two different types of soil texture coupled with five different soil profiles. Similarly, four scenarios were considered for the field experiments with five different types of soil texture couple with eight different soil profiles. The simulated infiltration rates and cumulative infiltrations were found to vary with soil layer change scenarios. The simulated cumulative infiltrations, ponding times, infiltrating rates at ponding, and total depth of wetting front at ponding of a five-layered laboratory soil column were identical for the three scenarios. Simulated cumulative infiltrations were 33.16, 23.65, 21.29, and 42.77 cm, respectively, for scenarios (combinations) 1, 2, 3, and 4 in the eight-layered soil profile in the field scenarios. Infiltration rates among scenarios at ponding were identical (0.46 to 0.53 cm/h) with field scenario data.

Copyright ©2022 IJAS. All rights reserved.

Keywords:

HYDROL-INF; Infiltration Rates; Modified Green Ampt; Ponding Condition; Soil Texture

1. Introduction

Green-Ampt Model (GAM) presented an approach for estimating infiltration into the soil and was developed based on fundamental physics (Green and Ampt, 1911). The conceptual representation of the infiltration process was based on Darcy's Law (McCuen, 1998). The output results of this model matched with the empirical observations dual assumptions for developing the GAM are 1) the ground surface is ponded by water (fully saturated), and 2) the actual rate of infiltration always equal to the infiltration capacity of the soil. The ponded water depth is small and negligible.

This condition indicates that the Green-Ampt model is applicable only when the rainfall intensity is greater than the infiltration rate (Almedeji and Esen, 2014; Zema et al., 2017). Therefore, researchers worldwide have been searching for new model/tool to satisfy these conditions. A good number of modifications work on GAM were reviewed by Broadbridge and White (1987); Cao et al., 2019; Chen et al., 2019; Zhang et al., 2020). Chu and Morino (2005) introduced the Modified Green-Ampt Model (MGAM) model along with algorithm for computing infiltration into the layered soils. This model eliminated those aforesaid problems. Moreover, the user interface of MGAM is simple and user-friendly Windows based which referred as HYDROL-INF (Version 5.03) and was developed for simulating infiltration and surface runoff (Chu and Morino, 2006; Chu, 2017). The important features of HYDROL-INF are that it can simulate 1) steady rainfall, unsteady rainfall, and multiple rainfall events (continuous simulation for combined wet and dry time periods); 2) consider homogeneous soil and layered soils; and 3) address uniform and variable initial soil moisture distribution conditions.

Infiltration refers to the process by which precipitation moves down through the Earth's surface and replenishes soil moisture, recharges reservoirs, and ultimately supports currents during dry periods (Viessman and Gary, 2003). It is a complicated process because of the irregularity in soil texture. Hydraulic properties including texture, bulk density, moisture contents (initial, residual, and saturated) of different soil layers and their arrangement/sitting order may have significant influence/impact on infiltration. While a wetting front passing through the interface of two dissimilar textured soil layers, the sudden change in soil hydraulic properties along with texture will make certain adjustment to water flow conditions in order to reach a new internal equilibrium (Chu and Marino, 2005). In case of water movement from coarse to fine soils and when the wetting front first reaches the fine textured soil, the infiltration rates may be slightly increased as a thin layer is wetted due to the greater attraction for water of the underlying finer soil because the finer soil generally has higher suction head and then resistance to flow owing to the fineness of the pores may be so great that flow is markedly reduced (Miller and Gardner, 1962; Chu and Marino, 2005). Therefore, the study was done with an objective of investigating the influence of changing soil layers (soil textures) on the infiltration rates and cumulative filtrations using secondary data for both laboratory and field settings. The hypothesis was that the MGAM model in the HYDROL-INF simulation software will be able to track the variations in infiltration rates and cumulative infiltration in varying soil textures combined with soil layer rearrangement.

2. Materials and Methods

Data inputs for HYDROL-INF simulation model were collected from a published article experiment conducted by Ma et al. (2011). Various parameters of this study were adopted and were considered as Scenario 1 and Scenario 4 for the laboratory and field conditions of this work, respectively (Table 2 and Table 5). A total seven scenarios were simulated in the study. To mimic the spatial variations of soil stratification in the real world, this study considered different layer arrangements in laboratory and field condition. For the sake of simplification of the research the made the following assumption: in spite of the fact that soil texture and stratification affect percolation rates, since estimating percolation rates was outside the purview of this study, percolation rates were only considered as affecting infiltration rates. For other Scenarios- Scenarios 2-3 and Scenarios 5-7- those parameters were rearranged and

modified (Table 3-4 and Table 6-8). For the laboratory situations, the soil profile consisted of five layers under infiltration with a constant water head. The soil column consisted of five layers with varying thickness of fine-textured to coarse layers and arranged in three different orders referred as scenarios (Table 1-3). The model input parameters including initial (θ_i), saturated (θ_s), and residual (θ_r) soil water contents, suction head (h_s), and saturated hydraulic conductivities (K_s) were kept constant for each particular soil layer. Other parameters for MGAM, such as soil water retention parameters (n and α) were obtained from Parameter-Estimation menu of the HYDROL-INF software. Additionally, effective hydraulic conductivities (K_e) for different soil types were assumed as $0.5 \times K_s$. The study assumed that each soil layer was homogeneous with uniform initial water content, and that the soil was evenly wetted by infiltration. In this study, steady state rainfall event was considered since a constant head was maintained at the soil surface for this study. All those data were fed into the HYDROL-INF Version 5.03 following the sequence showing in the flow chart (Figure 1). Duration of infiltration, cumulative infiltration and rate used in the study showed in (Table 1). After running all simulations with different scenarios, output results were analyzed and compared.

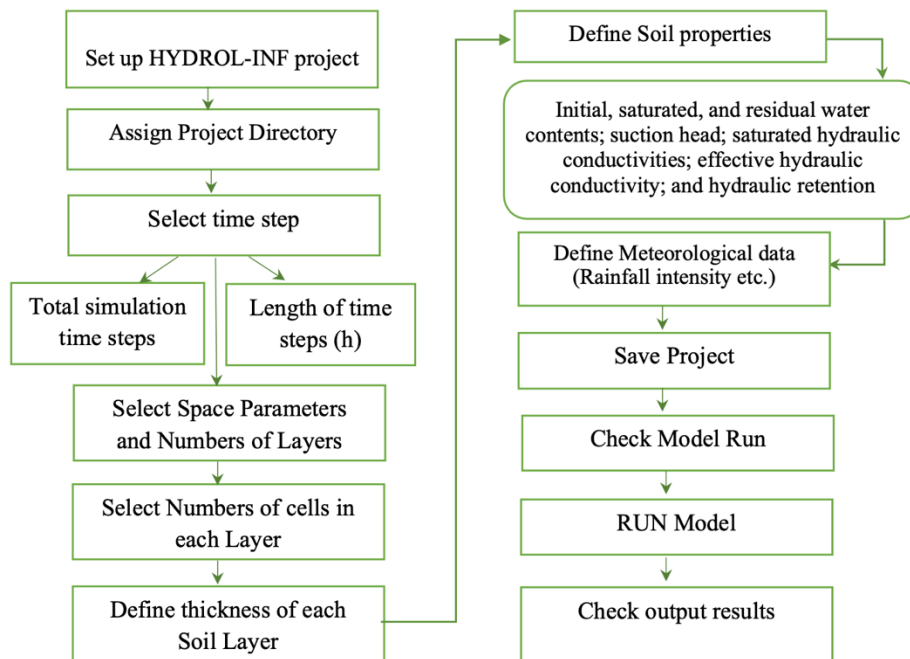


Figure 1. Flow chart of the research work.

Table 1. Brief description of the study used for simulations

	Field Scenario	Laboratory Scenario
Duration of infiltration (minute)	5,760	4,408
Cumulative Infiltration (cm)	51.4	73.1
Rate of infiltration (cm/h)	0.535	0.995

HYDROL-INF is a powerful Windows based software that can use either the GAM or MGAM method to simulate infiltration and surface runoff using steady/unsteady multiple rainfall events on layered soils with uniform or variable initial soil moisture conditions. To simulate infiltration in layered soil, the software also considers percolation, position of the wetting front, infiltration rate at pre- and post-ponding conditions, and ponding time and depth. The MGAM approach was used in this study to simulate infiltration into nonuniform soil layers and compute the infiltration rate at the wetting front as well as under pre-ponding and ponding conditions (Chu and Marino, 2005). All the equations used in this study, through HYDROL-INF, are available for interested readers in Chu and Marino's article (Chu & Marino, 2005).

Table 2. Different soil parameters (Ma et al., 2011) collected from parameter estimation menu of HYDROL-INF (Scenario 1 Lab)

Layer	Soil depth (cm)	Texture	Bulk Density g/cm ³	Initial Water Content θ_i (cm ³ /cm ³)	Saturated Water Content θ_s (cm ³ /cm ³)	Residual Water Content θ_r (cm ³ /cm ³)	Saturated Hydraulic Conductivity K_s (cm/h)	Effective Hydraulic Conductivity K_e (cm/h) (0.5K _s)	Suction Head h_s (cm)	Soil-Water Retention Parameter (n)	Soil-Water Retention Parameter (a)
1	100	Silt loam	1.4	0.16	0.5	0.067	0.876	0.438	52.74	1.41	0.02
2	20	Loam	1.37	0.14	0.51	0.078	1.152	0.576	25.97	1.56	0.036
3	30	Silt loam	1.46	0.16	0.46	0.067	0.756	0.378	53.59	1.41	0.02
4	30	Loam	1.5	0.19	0.5	0.078	0.306	0.153	29.87	1.56	0.036
5	120	Silt loam	1.5	0.13	0.49	0.067	0.798	0.399	73.86	1.41	0.02

Table 3. Different soil parameters (modified Ma et al., 2011) collected from parameter estimation menu of HYDROL-INF (Scenario 2 Lab)

Layer	Soil depth (cm)	Texture	Bulk Density g/cm ³	Initial Water Content θ_i (cm ³ /cm ³)	Saturated Water Content θ_s (cm ³ /cm ³)	Residual Water Content θ_r (cm ³ /cm ³)	Saturated Hydraulic Conductivity K_s (cm/h)	Effective Hydraulic Conductivity K_e (cm/h) (0.5K _s)	Suction Head h_s (cm)	Soil-Water Retention Parameter (n)	Soil-Water Retention Parameter (a)
1	100	Silt loam	1.4	0.16	0.5	0.067	0.876	0.438	52.74	1.41	0.02
2	120	Silt loam	1.5	0.13	0.49	0.067	0.798	0.399	73.86	1.41	0.02
3	30	Silt loam	1.46	0.16	0.46	0.067	0.756	0.378	53.59	1.41	0.02
4	20	Loam	1.37	0.14	0.51	0.078	1.152	0.576	25.97	1.56	0.036
5	30	Loam	1.5	0.19	0.5	0.078	0.306	0.153	29.87	1.56	0.036

Table 4. Different soil parameters (modified Ma et al., 2011) collected from parameter estimation menu of HYDROL-INF (Scenario 3 Lab)

Layer	Soil depth (cm)	Texture	Bulk Density g/cm ³	Initial Water Content θ_i (cm ³ /cm ³)	Saturated Water Content θ_s (cm ³ /cm ³)	Residual Water Content θ_r (cm ³ /cm ³)	Saturated Hydraulic Conductivity K_s (cm/h)	Effective Hydraulic Conductivity K_e (cm/h) (0.5K _s)	Suction Head h_s (cm)	Soil-Water Retention Parameter (n)	Soil-Water Retention Parameter (a)
1	20	Loam	1.37	0.14	0.51	0.078	1.152	0.576	25.97	1.56	0.036
2	30	Loam	1.5	0.19	0.5	0.078	0.306	0.153	29.87	1.56	0.036
3	100	Silt loam	1.4	0.16	0.5	0.067	0.876	0.438	52.74	1.41	0.02
4	30	Silt loam	1.46	0.16	0.46	0.067	0.756	0.378	53.59	1.41	0.02
5	120	Silt loam	1.5	0.13	0.49	0.067	0.798	0.399	73.86	1.41	0.02

Table 5. Different soil parameters (Ma et al., 2011) collected from parameter estimation menu of HYDROL-INF (Scenario 1 Field)

Layer	Soil depth (cm)	Texture	Bulk Density g/cm ³	Initial Water Content θ_i (cm ³ /cm ³)	Saturated Water Content θ_s (cm ³ /cm ³)	Residual Water Content θ_r (cm ³ /cm ³)	Saturated Hydraulic Conductivity K_s (cm/h)	Effective Hydraulic Conductivity K_e (cm/h) (0.5K _s)	Suction Head h_s (cm)	Soil-Water Retention Parameter (n)	Soil-Water Retention Parameter (a)
1	20	Clay loam	1.12	0.16	0.5	0.09	1.14	0.57	21.95	1.31	0.019
2	20	Clay loam	1.16	0.2	0.51	0.09	0.78	0.39	21.96	1.31	0.019
3	50	Silt clay loam	1.46	0.19	0.48	0.09	0.27	0.135	13.44	1.23	0.01
4	40	Silt loam	1.57	0.23	0.39	0.07	0.318	0.159	28.81	1.41	0.02
5	60	Silt clay loam	1.6	0.22	0.43	0.04	0.264	0.132	78.77	1.23	0.01
6	20	Loam	1.62	0.23	0.42	0.06	0.432	0.216	99.23	1.56	0.036
7	30	Loam sand	1.64	0.15	0.4	0.03	4.02	2.01	48.96	2.28	0.124
8	40	Silt loam	1.48	0.16	0.44	0.05	0.924	0.462	119.22	1.41	0.02

Table 6. Different soil parameters (modified Ma et al., 2011) collected from parameter estimation menu of HYDROL-INF (Scenario 2 Field)

Layer	Soil depth (cm)	Texture	Bulk Density g/cm ³	Initial Water Content θ_i (cm ³ /cm ³)	Saturated Water Content θ_s (cm ³ /cm ³)	Residual Water Content θ_r (cm ³ /cm ³)	Saturated Hydraulic Conductivity K_s (cm/h)	Effective Hydraulic Conductivity K_e (cm/h) (0.5K _s)	Suction Head h_s (cm)	Soil-Water Retention Parameter (n)	Soil-Water Retention Parameter (a)
1	50	Silt clay loam	1.46	0.19	0.48	0.04	0.27	0.135	13.44	1.23	0.01
2	60	Silt clay loam	1.6	0.22	0.43	0.09	0.264	0.132	78.77	1.23	0.01
3	40	Silt loam	1.57	0.23	0.39	0.05	0.318	0.159	28.81	1.41	0.02
4	40	Silt loam	1.48	0.16	0.44	0.07	0.924	0.462	119.22	1.41	0.02
5	30	Loam sand	1.64	0.15	0.4	0.03	4.02	2.01	48.96	2.28	0.124
6	20	Loam	1.62	0.23	0.42	0.04	0.432	0.216	99.23	1.56	0.036
7	20	Clay loam	1.12	0.16	0.5	0.09	1.14	0.57	21.95	1.31	0.019
8	20	clay loam	1.16	0.2	0.51	0.09	0.78	0.39	21.96	1.31	0.019

Table 7. Different soil parameters (modified Ma et al., 2011) collected from parameter estimation menu of HYDROL-INF (Scenario 3 Field)

Layer	Soil depth (cm)	Texture	Bulk Density g/cm ³	Initial Water Content θ_i (cm ³ /cm ³)	Saturated Water Content θ_s (cm ³ /cm ³)	Residual Water Content θ_r (cm ³ /cm ³)	Saturated Hydraulic Conductivity K_s (cm/h)	Effective Hydraulic Conductivity K_e (cm/h) (0.5K _s)	Suction Head h_s (cm)	Soil-Water Retention Parameter (n)	Soil-Water Retention Parameter (a)
1	50	Silt clay loam	1.46	0.19	0.48	0.09	0.27	0.135	13.44	1.23	0.01
2	20	Clay loam	1.12	0.16	0.5	0.09	1.14	0.57	21.95	1.31	0.019
3	40	Silt loam	1.48	0.16	0.44	0.05	0.924	0.462	119.22	1.41	0.02
4	60	Silt clay loam	1.6	0.22	0.43	0.04	0.264	0.132	78.77	1.23	0.01
5	30	Loam sand	1.64	0.15	0.4	0.03	4.02	2.01	48.96	2.28	0.124
6	40	Silt loam	1.57	0.23	0.39	0.07	0.318	0.159	28.81	1.41	0.02
7	20	clay loam	1.16	0.2	0.51	0.09	0.78	0.39	21.96	1.31	0.019
8	20	Loam	1.62	0.23	0.42	0.09	0.432	0.216	99.23	1.56	0.036

Table 8. Different soil parameters (modified Ma et al., 2011) collected from parameter estimation menu of HYDROL-INF (Scenario 4 Field)

Layer	Soil depth (cm)	Texture	Bulk Density g/cm ³	Initial Water Content θ_i (cm ³ /cm ³)	Saturated Water Content θ_s (cm ³ /cm ³)	Residual Water Content θ_r (cm ³ /cm ³)	Saturated Hydraulic Conductivity K_s (cm/h)	Effective Hydraulic Conductivity K_e (cm/h) (0.5K _s)	Suction Head h_s (cm)	Soil-Water Retention Parameter (n)	Soil-Water Retention Parameter (a)
1	20	Loam	1.62	0.23	0.42	0.09	0.432	0.216	99.23	1.56	0.036
2	30	Loam sand	1.64	0.15	0.4	0.03	4.02	2.01	48.96	2.28	0.124
3	40	Silt loam	1.48	0.16	0.44	0.05	0.924	0.462	119.22	1.41	0.02
4	40	Silt loam	1.57	0.23	0.39	0.07	0.318	0.159	28.81	1.41	0.02
5	20	Clay loam	1.12	0.16	0.5	0.09	1.14	0.57	21.95	1.31	0.019
6	20	Clay loam	1.16	0.2	0.51	0.09	0.78	0.39	21.96	1.31	0.019
7	50	Silt clay loam	1.46	0.19	0.48	0.04	0.27	0.135	13.44	1.23	0.01
8	60	Silt clay loam	1.6	0.22	0.43	0.09	0.264	0.132	78.77	1.23	0.01

3. Results and Discussion

3.1 Infiltration rate for three different scenarios

The physical characteristics (parameters) of the soil layers for the laboratory column and field profile are shown in Tables 2 and 5, respectively (Ma et al., 2011). Additional input data for residual water content, effective hydraulic conductivity, suction head, and soil-water retention parameters were taken from the HYDROL-INF simulation platform (Chu and Marino, 2006) This study examined changing the soil layers to simulate the spatial variability of soil layers in actual settings shown in Tables 2 and 5 and observing their subsequent effect on soil-water flow using the HYDROL-INF platform. Tables 1 to 3 show scenarios 1 to 3 for the lab condition. Tables 4–7 displayed the field condition scenarios 1–4 in the same manner.

The infiltration rate is significantly influenced by several aspects of soil, particularly its texture. Infiltration rates for three different scenarios (changing soil textures) in the laboratory soil column and four different scenarios in the field soil layers are analyzed in Figures 2 and 3, respectively. For laboratory setup, in Scenario 1, with alternate silt loam and loam soil layers with different layer thickness up to 300 cm soil profile showed sudden decrease and increase in infiltration rates from coarse to relatively fine textured soil layers and from fine to relatively coarse textured soil layers, respectively. For example, the curve of Scenario 1 in Figure 2 repeatedly reversed its direction as the infiltration rate increased for silty loam to loam soil (i.e. from fine to coarse in texture) and vice versa. In contrast, Scenario 2 showed a uniform decrease in infiltration rates until it reached a soil layer with a different texture, despite having three distinct sub-layers with a combined thickness of 250 cm. And when the soil texture changed to a relatively coarse one (loam) at the end of those three distinct sub-layers (silt loam), the rate of infiltration suddenly increased. The results of this study were consistent with

those of Bean and Dukes (2016); and Schifman and Shuster (2019). In Scenario 3, however, water movement shifting from a layer of loam soil (coarse) to a layer of silt loam (fine) textured soil slightly increased infiltration rates for a short period of time before there were the typical decreasing trends. This might be a result of the soil's second- and third-layers' initial soil water content (Fouli et al., 2013) and effective hydraulic conductivity (Sacha et al., 2019). The effective hydraulic conductivity of the second layer was much lower (0.306 cm/h) than that of the silt loam (0.876 cm/h), and the initial soil water content of the loam (second layer) was higher ($0.19 \text{ cm}^3/\text{cm}^3$) than that of silt the loam (third layer) ($0.16 \text{ cm}^3/\text{cm}^3$).

Similarly, in the field soil column, the soil profile consisted of eight layers under infiltration with a constant water head. The soil columns with varying thickness of fine-textured to coarse layers and arranged in four different orders referred as scenarios (Table 5 -8). Figure 3 showed the simulated infiltration rates for four different scenarios (changing soil textures) in the field soil layers. In Scenarios 1 to 4 with field soil profile, four combinations of soil layers with different textures were considered for investigating their effects on infiltration rates.

In the field setting, in Scenario 1, infiltration started 25 hours after the initiation of the experiment and showed a uniform reduction in infiltration rates over time up to 73 hours. Following that, there was a sharp increase in infiltration rate, most likely due to entering the coarse (sandy loam to silt loam) soil layer, and it gradually decreased or return to equilibrium. In Scenario 2, infiltration rates showed a uniform decrease up to 63 hours. When the texture changed from loam to silt loam, there was a sudden increase in infiltration rate of up to 0.35 cm/h. Then, infiltration rates started decreasing (reaching equilibrium) again in the clay loam layers (Figure 3). Similar to Scenario 2, infiltration rates in Scenario 3 showed a uniform decrease up to 63 hours. When the soil texture changed from silty loam to loam, the infiltration rate changed dramatically. In scenario 4, infiltration started decreasing 43 hours after the initiation of the experiment and showed a uniform reduction in infiltration rates over time up to 57 hours. After that, there was a slight increase in infiltration rate, most likely due to entering relatively fine textured (clay loam and silty clay loam) soil layers, and started decreasing again.

In scenario 1, the infiltration rates decreased uniformly from the comparatively coarse fifth soil layer to the sixth soil layer (from silty-clay loam to loam). The infiltration began to increase at that point and then gradually decreased after that (Saxton et al., 1986). Similar to Scenario 1, Scenario 2 displayed a regular descending trend until it reached a relatively coarser loam soil (from layer 4 to layer 5). At that time, the infiltration rate suddenly increased, and it then resumed its usual downward trend (Figure 3). The infiltration began to increase at that point and then gradually decreased after that (Schifman and Shuster, 2019). Both field and laboratory settings, soil texture played a substantial role in determining infiltration rate. Furthermore, compared to a laboratory setting, these natural field settings did not exhibit a sharp rise and fall in infiltration rate.

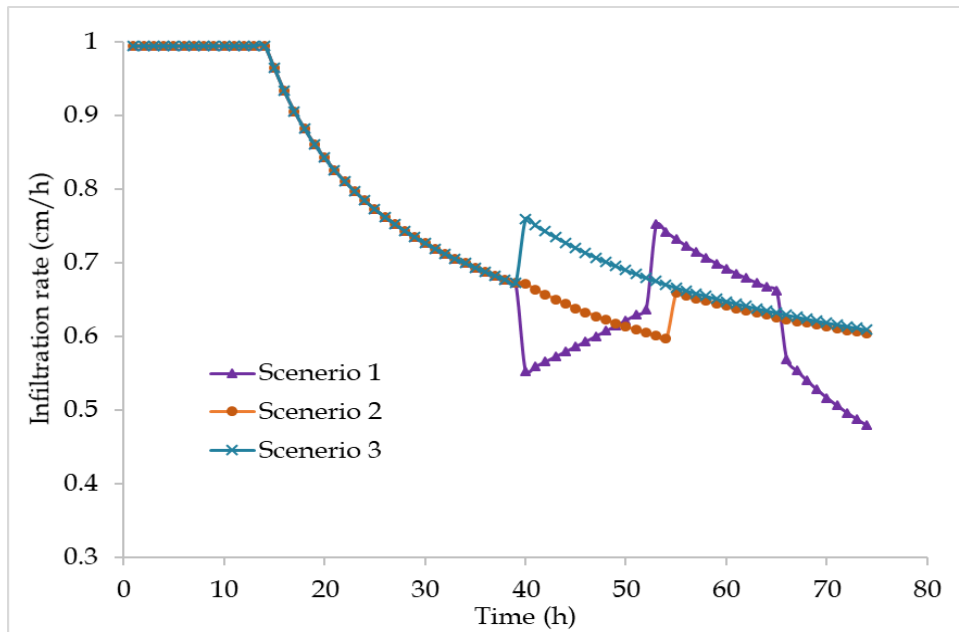


Figure 2. Comparison of simulated infiltration rates for three different scenarios (changing soil textures) in the laboratory soil column.

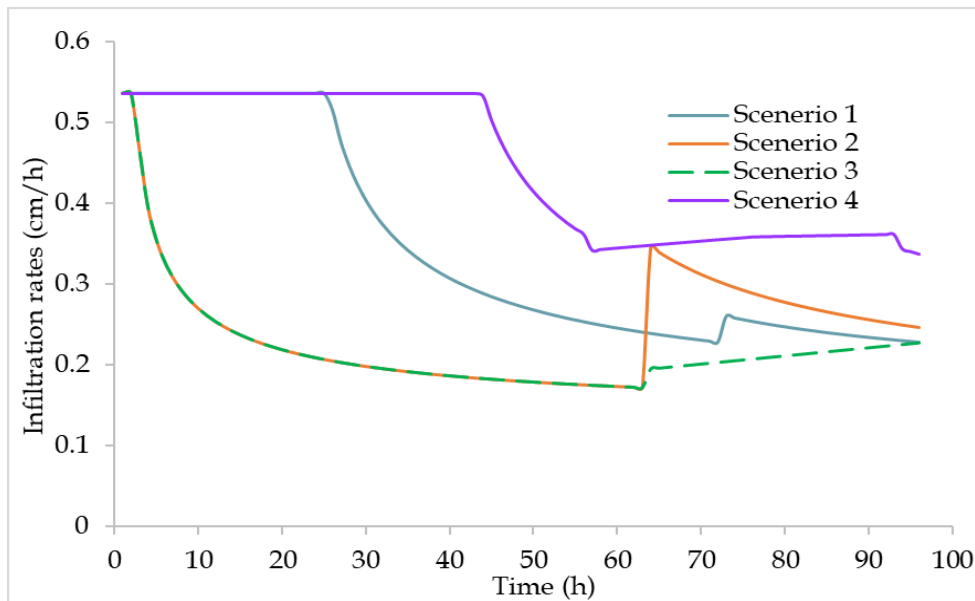


Figure 3. Comparison of simulated infiltration rates for four different scenarios (changing soil textures) in the field soil layers.

3.2 Cumulative infiltration rate for those scenarios

Figure 4 and 5 showed the comparison of cumulative infiltration, respectively, for three different scenarios (changing soil textures) in the laboratory soil column and four different scenarios in the field setting. Additionally, simulated cumulative infiltrations, ponding times, infiltrating rates at ponding, and total depth of wetting front at ponding were identical for five layers laboratory soil column with two different soil textures as presented in Table 9.

Table 9. Comparison of simulated infiltrations parameters for three scenarios using data collected from laboratory soil column experiment

Performance Parameters	Scenario 1	Scenario 2	Scenario 3
Cumulative Rainfall (cm)	73.63	73.63	73.63
Cumulative Runoff (cm)	18.52	18.08	16.81
Cumulative Infiltrations (cm)	55.11	55.54	56.81
Exact Ponding Time, I_p (h)	14.17	14.17	14.17
Runoff Initiation Time (between hours)	14 - 15	14 - 15	14 -15
Depth of wetting front at Ponding (cm)	41.47	41.47	41.47
Cumulative Infiltration at ponding (cm)	14.91	14.91	14.91
Infiltration Rate at Ponding (cm/h)	0.9647	0.9647	0.9647
Total Depth of Wetting Front at Ponding (cm)	165.18	164.85	165.87

The comparison of simulated cumulative infiltrations was displayed in Figures 4 and 5, respectively, for three different scenarios (changing soil textures) in the laboratory setting and four different scenarios in the field. For Scenarios 1 through 3, three combinations of soil layers with different textures were considered in a lab setting to examine their effects on cumulative infiltrations. A general trend of gradual growth has been seen. Among those three, Scenario 3 demonstrated the greatest cumulative infiltration, while Scenario 2 revealed the least amount. These outcomes were in line with the variation in soil texture found in the soil profile. In Scenario 3, the upper soil layer contained coarser soil layers, which contributed to a rise in cumulative infiltration. The study supported the results of Kale and Sahoo (2011). Therefore, cumulative infiltration was greatly impacted by the arrangement of soil layers (Figure 4).

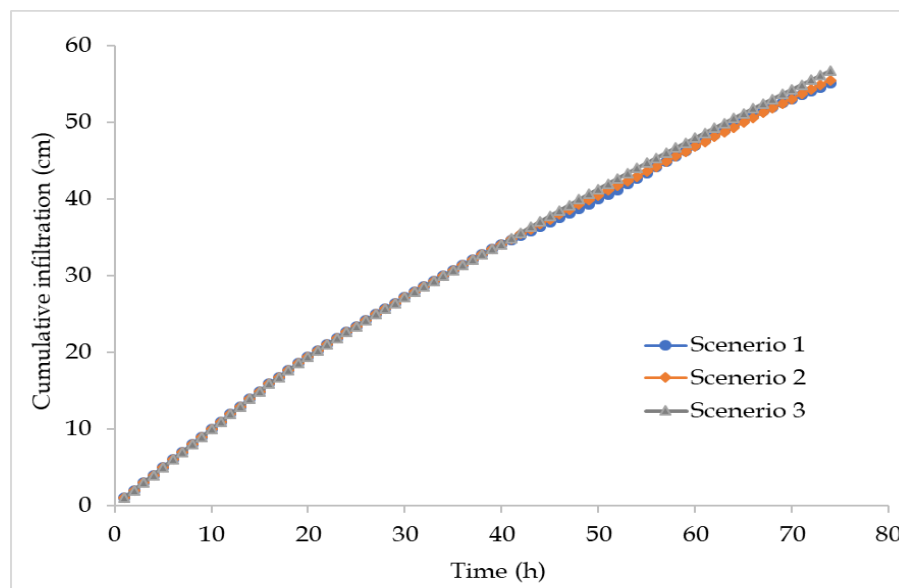


Figure 4. Comparison of simulated cumulative infiltrations for three different scenarios (changing soil textures) in the laboratory soil layers.

For field setting, simulated cumulative infiltrations, ponding times, infiltrating rates at ponding, and total depth of wetting front at ponding were differ substantially due to reengagement of soil layers as presented in Table 10. Simulated cumulative infiltrations were 33.16, 23.65, 21.29, and 42.77 cm, respectively, for scenarios 1, 2, 3, and 4 using eight layered soil profile in the field (Figure 5). Similarly, exact ponding times were 25.25, 2.45, 2.45, and 44 hours, respectively, for scenarios 1, 2, 3, and 4. The total depth of wetting from at ponding were 125, 94, 70, and 173 cm respectively, for scenarios 1, 2, 3, and 4. However, infiltration rates among scenarios at ponding were identical (Table 10).

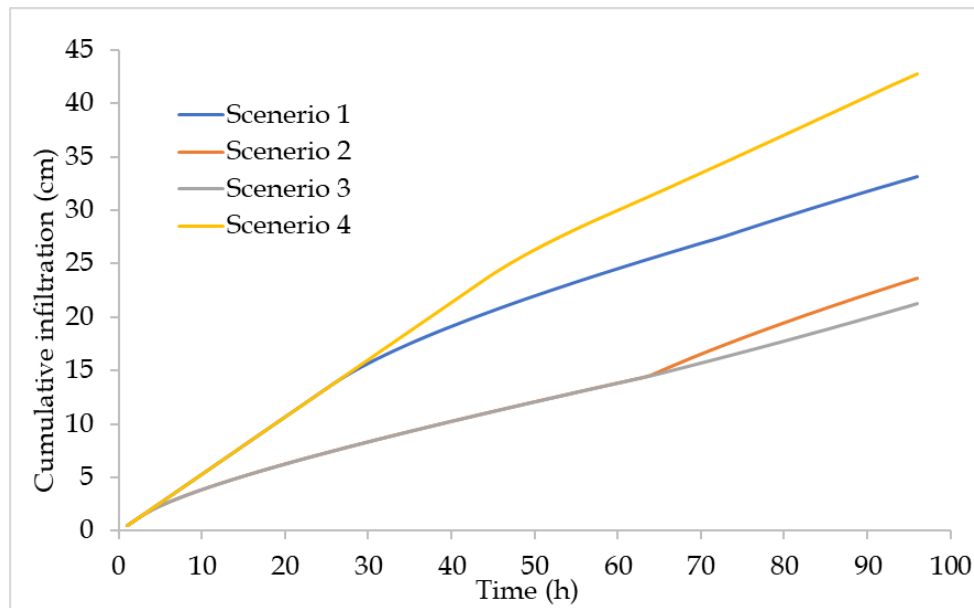


Figure 5. Comparison of simulated cumulative infiltrations for four different scenarios (changing soil textures) in the field soil layers.

Figure 5 depicts the cumulative infiltrations that were simulated in a field setting for four different scenarios (changing soil textures). For Scenarios 1 through 4, eight combinations of soil layers with different textures were considered in a field setting to examine their effects on cumulative infiltrations. For all four scenarios, there has been a general trend toward slow growth. However, out of all the scenarios, Scenario 4 demonstrated the greatest cumulative infiltration, whereas Scenario 3 demonstrated the least. These outcomes were caused by the arrangement of the soil layers and were comparable to those of Mazaheri and Mahmoodabadi (2012). For Scenario 4, the top few layers comprised of coarser soil, which assisted in the initial stage's increase in cumulative infiltration. In Scenario 3, however, the top few layers were composed of finer soil, which was the reason for lower cumulative infiltration.

Table 10. Comparison of simulated infiltrations parameters for four scenarios using data collected from field experiment.

Performance Parameters	Scenario 1	Scenario 2	Scenario 3	Scenario 4
Cumulative Rainfall (cm)	51.39	51.39	51.39	51.39
Cumulative Runoff (cm)	18.23	27.74	30.10	8.62
Cumulative Infiltrations (cm)	33.16	23.65	21.29	42.77
Exact Ponding Time, I_p (h)	25.25	2.454	2.454	43.90
Runoff Initiation Time (between hours)	25-26	2-3	2-3	43-44
Depth of wetting front at Ponding (cm)	43.16	5.47	5.47	96.29
Cumulative Infiltration at ponding (cm)	13.91	1.58	1.58	23.55
Infiltration Rate at Ponding (cm/h)	0.5156	0.4668	0.4668	0.5321
Total Depth of Wetting Front at Ponding (cm)	125.39	93.58	69.99	173.02

4. Conclusion

In general, this study found an abrupt decrease and increase in infiltration rate from fine to relatively coarse textured soil layers. Simulated cumulative infiltrations, ponding times, infiltrating rates at ponding, and total depth of wetting front at ponding were identical for three scenarios in the five layered laboratory soil columns. In contrast, for field soil profile, simulated cumulative infiltrations, ponding times, infiltrating rates at ponding, and total depth of wetting front at ponding differed substantially due to rearrangement of soil layers. The study revealed that the MGAM model in the HYDROL-INF simulation software successfully track the variations in infiltration rates and cumulative infiltration in varying soil textures combined with soil layer rearrangement.

Acknowledgements

Corresponding author acknowledges the National Agricultural Technology Program-Phase II Project (NATP-2), BARC, Dhaka, Bangladesh for financial support of her study.

References

- Almedeij, J. and I.I. Esen. (2014). Modified Green-Ampt infiltration model for steady rainfall. *Journal of Hydrologic Engineering*, 19(9): 04014011-7. DOI: 10.1061/(ASCE)HE.1943-5584.0000944.
- Bean, E.Z. and M.D. Dukes. (2016). Evaluation of infiltration basin performance on coarse soils. *Journal of Hydrologic Engineering*, 21(1): 04015050.
- Broadbridge, P. and I. White. (1987). Time to ponding: Comparison of analytic, quasi-analytic, and approximate predictions. *Water Resour. Res.*, 23(12): 2302-2310. DOI: 10.1029/WR023i012p02302.

- Cao, D.F., B. Shi, H.H. Zhu, H. Inyang, G.Q. Wei, Y. Zhang and C.S. Tang. (2019). Feasibility investigation of improving the modified Green-Ampt model for treatment of horizontal infiltration in soil. *Water*, 11(4): 645.
- Chen, S., X. Mao and C. Wang. (2019). A modified Green-Ampt model and parameter determination for water infiltration in fine-textured soil with coarse interlayer. *Water*, 11(4): 787.
- Chu, X (2017). HYDROL-INF modeling System [Computer software], Version 5.03. Dept of Civil, Construction and Environmental Engineering, North Dakota State University, Fargo, ND, USA.
- Chu, X. and M.A. Mariño. (2005). Determination of ponding condition and infiltration into layered soils under unsteady rainfall. *Journal of Hydrology*, 313(3-4): 195-207. DOI: 10.1016/j.jhydrol.2005.03.002.
- Chu, X. and M.A. Mariño. (2006). Simulation of infiltration and surface runoff: a windows-based hydrologic modeling system HYDROL-INF. In World Environmental and Water Resource Congress 2006: Examining the Confluence of Environmental and Water Concerns, 1-8. DOI: [https://doi.org/10.1061/40856\(200\)429](https://doi.org/10.1061/40856(200)429).
- Fouli, Y., B.J. Cade-Menun and H.W. Cutforth. (2013). Freeze-thaw cycles and soil water content effects on infiltration rate of three Saskatchewan soils. *Canadian Journal of Soil Science*, 93(4): 485-496. DOI: 10.4141/cjss2012-060.
- Green, W.H. and G. Ampt. (1911). Studies of soil physics, part I - the flow of air and water through soils. *J. Ag. Sci.*, 4:1-24. DOI: 10.1017/S0021859600001441.
- Ma, Y., S. Feng, H. Zhan, X. Liu, D. Su, S. Kang and X. Song. (2011). Water infiltration in layered soils with air entrapment: modified Green-Ampt model and experimental validation. *Journal of Hydrologic Engineering*, 16(8): 628-638. DOI: 10.1061/(ASCE)HE.1943-5584.0000360.
- Mazaheri, M.R. and M. Mahmoodabadi. (2012). Study on infiltration rate based on primary particle size distribution data in arid and semiarid region soils. *Arabian Journal of Geosciences*, 5(5): 1039-1046. DOI: 10.1007/s12517-011-0497-y.
- McCuen, R.H. (1998). Hydrologic analysis and design. Prentice Hall, Upper Saddle River, NJ, USA.
- Miller, D.E. and W.H. Gardner. (1962). Water infiltration into stratified soil. *Soil science society of America Journal*, 26(2): 115-119. DOI: 10.2136/sssaj1962.03615995002600020007x.
- Kale, R.V. and B. Sahoo. (2011). Green-Ampt infiltration models for varied field conditions: A revisit. *Water resources management*, 25(14): 3505-3536. DOI:10.1007/s11269-011-9868-0.
- Sacha, J., M. Snehota, P. Trtik and J. Hovind. (2019). Impact of infiltration rate on residual air distribution and hydraulic conductivity. *Vadose Zone Journal*, 18(1): 1-15. DOI: <https://doi.org/10.2136/vzj2019.01.0003>
- Saxton, K.E., W. Rawls, J.S. Romberger and R.I. Papendick. (1986). Estimating generalized soil-water characteristics from texture. *Soil science society of America Journal*, 50(4): 1031-1036. DOI: 10.2136/sssaj1986.03615995005000040039x.

- Schifman, L.A., and W.D. Shuster. (2019). Comparison of measured and simulated urban soil hydrologic properties. *Journal of hydrologic engineering*, 24(1). DOI: 10.1061/(ASCE)HE.1943-5584.0001684.
- Viessman, W.J., and L.L. Gary. (2003). *Introduction to Hydrology*. Prentice Hall, Upper Saddle River, NJ, USA.
- Zhang, Q., W. Chen and Y. Kong. (2020). Modification and discussion of the Green-Ampt model for an evolving wetting profile. *Hydrological Sciences Journal*, 65(12): 2072-2082.
- Zema, D.A., A. Labate, D. Martino and S.M. Zimbone. (2017). Comparing different infiltration methods of the HEC-HMS model: the case study of the Mésima Torrent (Southern Italy). *Land Degradation & Development*, 28(1): 294-308.